Published in *Langmuir* (2012) **28**: 299-306

The hydrogen bonding-driven self-assembly of PEGylated organosilica nanoparticles with poly(acrylic acid) in aqueous solutions and in layer-by-layer deposition at solid surfaces

Galiya S. Irmukhametova[†,‡] *, Brian J. Fraser*[§]*, Joseph L. Keddie*[§]*,*

Grigoriy A. Mun[‡]*, Vitaliy V. Khutoryanskiy**[†]

[†]Reading School of Pharmacy, University of Reading, Whiteknights, P.O. Box 224, RG6 6AD Reading, United Kingdom. Fax: +44 (0) 118 378 4703; Tel: +44 (0) 118 378 6119; E-mail: v.khutoryanskiy@reading.ac.uk

[‡]Department of Colloidal and Macromolecular Chemistry, al-Farabi Kazakh National University, 71 al-Farabi avenue, Almaty, Kazakhstan.

[§]Department of Physics, University of Surrey, GU2 7XH Guildford, United Kingdom

RECEIVED DATE

Published in *Langmuir* (2012) **28**: 299-306

ABSTRACT: PEGylated organosilica nanoparticles have been synthesized through self-condensation of 3-mercaptopropyltrimethoxysilane in dimethylsulfoxide into thiolated nanoparticles with their subsequent reaction with methoxypolyethylene glycol maleimide. The PEGylated nanoparticles showed excellent colloidal stability over a wide range of pHs in contrast to the parent thiolated nanoparticles, which have a tendency to aggregate irreversibly under acidic conditions (pH < 3.0). Due to the presence of a poly(ethylene glycol)-based corona, the PEGylated nanoparticles are capable of forming hydrogen-bonded interpolymer complexes with poly(acrylic acid) in aqueous solutions under acidic conditions, resulting in larger aggregates. The use of hydrogen-bonding interactions allows their more efficient attachment of the nanoparticles to surfaces. The alternating deposition of PEGylated nanoparticles and poly(acrylic acid) on silicon wafer surfaces in a layer-by-layer fashion leads to multilayered coatings. The self-assembly of PEGylated nanoparticles with poly(acrylic acid) in aqueous solutions and at solid surfaces was compared to the behavior of linear poly(ethylene glycol). The nanoparticle system creates thicker layers than the poly(ethylene glycol), and a thicker layer is obtained on a poly(acrylic acid) surface than on a silica surface, because of the effects of hydrogen bonding. Some implications of these hydrogen bonding-driven interactions between PEGylated nanoparticles and poly(acrylic acid) for pharmaceutical formulations are discussed.

Keywords: organosilica nanoparticles, PEGylation, poly(acrylic acid), interpolymer complexes, layer-by-layer deposition

Published in *Langmuir* (2012) **28**: 299-306

1. INTRODUCTION

Organosilica nano- and micro-particulate materials have received considerable attention in the past few decades due to their potential applications in catalysis,[1] separation technologies,[2] bioimaging[3] and drug delivery.[4] The approach frequently used for the synthesis of these materials was pioneered by Stöber et al.[5] It involves the hydrolysis of alkyl silicates with subsequent condensation of silicic acid in alcohol or alcohol-water media in the presence of a base (ammonia or sodium hydroxide) as a catalyst. The Stöber method has often been used for synthesis of organosilica particles through condensation of tetraethoxysilane (TEOS)[6,7] or TEOS co-condensation with other functional silanes, such as 3-aminopropyltriethoxysilane (APTS)[8-10] and 3-mercaptopropyltrimethoxysilane (MPTS).[10-12] The typical size of organosilica particles synthesized using Stöber conditions is often greater than 500 nm.[6,7,9] The Stöber method was also used to generate mesoporous materials, where homo- or co-condensation of TEOS with other functional silanes was conducted in the presence of low molecular weight or polymeric surfactants as a template.[1,10,13]

Fewer studies have reported the development of organosilica nanoparticles with sizes smaller than 200 nm. These nanoparticles could be of interest for drug delivery applications where their small size allows the penetration of certain biological barriers. The majority of previous studies aimed at preparation of sub-200 nm organosilica nanoparticles have used very high dilutions of silanes during the synthesis. For example, Nooney et al.[14] have reported the possibility of preparing the nanoparticles over a range of diameters from 65 to 740 nm from TEOS by varying the initial silicate and surfactant concentrations in dilute solutions.

Möller and co-workers[15] have reported the synthetic procedure leading to sub-200 nm TEOS-based mesoporous nanoparticles, where the common base NaOH was replaced with

triethanolamine. This change in reaction conditions resulted in the formation of discrete mesoporous nanoparticles with narrow size distributions from *concentrated* solutions. The authors[15] related this result to the possibility of conducting the reaction at lower pHs and to the effect of chelating properties of triethanolamine on the condensation.

Recently, we have reported a novel approach for the synthesis of sub-100 nm thiolated nanoparticles based on 3-mercaptopropyltrimethoxysilane (MPTS) from relatively concentrated solutions and demonstrated the feasibility of their fluorescent labeling and PEGylation.[16] The specific features of our novel synthetic methodology are the use of dimethylsulfoxide (DMSO) as a solvent medium combined with the presence of oxygen dissolved in the DMSO, resulting in the simultaneous condensation of siloxane groups and the formation of disulfide bridges due to thiol group oxidation. Thiolated MPTS nanoparticles were found to be strongly adhering to ocular mucosal surfaces, which is due to disulfide bridge formation between their thiol groups and cystein-rich domains in mucins. After PEGylation these nanoparticles lost their mucoadhesive properties. For a range of applications, there remains a need to control the assembly of nanoparticles in solution and at interfaces.

Here, we synthesized a series of PEGylated MPTS-based nanoparticles and studied their physicochemical characteristics in aqueous dispersions. It is established that PEGylation of MPTS-nanoparticles improves their aggregation stability over a wide range of solution pHs. The presence of PEG on the surface of these nanoparticles opens the unique possibility of their further modification through hydrogen bonding-driven interactions with poly(acrylic acid) under acidic conditions. We observe these interactions both in solutions and at a solution/solid interface, and we use them for building multilayered coatings utilizing a layer-by-layer deposition approach. Our use of hydrogen-bonding interactions between PEGylated

nanoparticles and poly(acrylic acid) allows their more efficient attachment to the surfaces. As shall be discussed later, the hydrogen bonding-driven interactions between PEGylated nanoparticles and poly(acrylic acid) have important implications for pharmaceutical formulations.

2. EXPERIMENTAL SECTION

2.1. Materials. 3-Mercaptopropyltrimethoxysilane (MPTS, 95%) was purchased from ABCR GmbH & Co. (Germany) and used without purification. Poly(acrylic acid) (PAA, MW 450,000), methoxyethylene glycol maleimide (MePEG, ≥90% (NMR), MW 5000), 5-iodoacetamido fluorescein (≥95% (HPLC)), 5,5'-dithiobis(2-nitrobenzoic acid) (DTNB, ≥98% (TLC), and cysteine hydrochloride were purchased from Sigma-Aldrich, Inc and used as received. Dimethyl sulfoxide and NaOH were laboratory grade reagents purchased from Fisher Scientific Ltd (UK).

2.2. **Synthesis of thiolated nanoparticles**. Thiolated nanoparticles were synthesized as described in our previous publication.[16] Briefly, 0.75 mL (0.7883 g) of MPTS was mixed with 20 mL of DMSO and 0.5 mL of 0.5 mol/L aqueous NaOH and stirred continuously using a magnetic stirrer. After 24 h of stirring the reaction mixture at room temperature, the nanoparticles were purified by dialysis.

2.3. Synthesis of PEGylated nanoparticles. PEGylated nanoparticles were synthesized by adding various quantities of MePEG to aqueous dispersions of thiolated MPTS-based nanoparticles and stirring these mixtures for 9 h. The nanoparticles were purified by dialysis.

2.4. Synthesis of thiolated nanoparticles labeled with a fluorescent dye. Fluorescent dye-labeled nanoparticles were synthesized as described in our previous study[16] by mixing 0.10 mg of 5-iodacetamido fluorescein with 1 mL of thiolated nanoparticles dispersion. The reaction mixture was stirred for 15 h at room temperature. The nanoparticles were purified by dialysis.

2.5. PEGylation of fluorescently-labeled nanoparticles. Fluorescently-labeled PEGylated nanoparticles were synthesized as described in our previous publication.[16] Briefly, 1 mL of aqueous dispersion of fluorescently-labeled thiolated nanoparticles were mixed with 20 mg of methoxyethylene glycol maleimide and the reaction mixture was stirred for 9 h at room temperature. The nanoparticles were purified by dialysis.

2.6. Purification and storage of nanoparticles. The nanoparticles were purified by dialysis against 5 L of deionized water for 48 h (8 changes of water in total). Dialysis tubing MWCO 12-14 kDa (Medicell Int. Ltd, UK) was used for this purpose. The purified nanoparticles were stored in aqueous dispersions in sealed containers in a refrigerator. The fluorescently-labeled nanoparticles were stored in a sealed vial wrapped in aluminum foil to avoid exposure to light.

2.7. Dynamic light scattering and zeta-potential measurements. Dynamic light scattering and zeta-potential measurements were conducted on dilute solutions of nanoparticles at 25 ºC using a Nano-S Zetasizer (Malvern Instruments, UK). Each sample was analyzed at least three times and the mean values of particle size, polydispersity index (PDI), and zeta-potential were calculated. Prior to dynamic light scattering studies the polymer solutions and dispersions of

PEGylated nanoparticles were filtered through 0.2 μm filters (Minisart, Sartorius UK). In this work z-size refers to z-average diameter of nanoparticles measured by dynamic light scattering.

2.8. Ellman's assay. The thiol groups content in nanoparticles was determined by Ellman's assay.[17] Before analysis, all nanoparticles were freeze-dried using a freeze-drier (Heto Power Dry LL 3000, Thermo Electron Corporation). 2 mg/ml of nanoparticle dispersions were prepared in 500 μL phosphate buffer solution (0.5 mol/L, pH 8) and were allowed to hydrate for 1 h. In the meantime, 3 mg of the Ellman's reagent or DTNB was dissolved in 10 mL of 0.5 mol/L phosphate buffer solution at pH 8. Then 500 μL of DTNB solution was added to 500 μL of nanoparticles and incubated in the dark for 90 min. After that, the nanoparticle dispersion was centrifuged for 10 min at 13,000 rpm (Sanyo, MSE Micro Centaur) and 300 μL of the supernatant was placed in a 96-well microlitre plate. Absorbance was measured at 405 nm with a plate reader (Spectra max 340 PC). The thiol concentration was calculated from a calibration curve of cysteine hydrochloride prepared as a series of solutions under the same conditions and with a concentration range of 0.020 – 0.793 μmol/mL.

2.9. Thermal gravimetric analysis (TGA) of nanoparticles. The dried thiolated and PEGylated nanoparticles were studied by TGA to determine the content of MePEG. This analysis was performed in the range of 25 - 1000 ºC at a heating rate of 10 ºC/min in a nitrogen atmosphere using TGA Q50 (TA Instruments Ltd, UK). The amount of MePEG in the nanoparticles was calculated by comparing the percentages of a solid residual obtained after reaching 1000 ºC for thiolated and PEGylated nanoparticles.

2.10. pH adjustment and measurements. The pH of nanoparticle dispersions was adjusted by adding small portions of either 1 mol/L HCl or 1 mol/L NaOH. The pH was measured using a pH-meter (SevenEasy, Mettler Toledo, Switzerland) at room temperature.

2.11. Preparation of PAA solutions. PAA was dispersed in deionized water to make 1 mg/mL, and the solution was left stirring overnight. Then the pH of this solution was adjusted to pH 2.96 by adding small portions of 1 mol/L HCl.

2.12. Formation of interpolymer complexes in solutions. Interpolymer complexes were prepared by mixing 1 mg/mL solutions of PAA with dispersions of PEGylated nanoparticles at pH 2.96 in 1:1 volume ratio. Dynamic light scattering experiments with interpolymer complexes were conducted 10 minutes after mixing interacting components.

2.13. Layer-by-layer deposition on silicon wafers and spectroscopic ellipsometry. Polished silicon (100) wafers were cut into small pieces (approximately 2 cm × 1.2 cm) using a diamond scribe. Each wafer was then treated in a UV-ozone atmosphere (BioForce Nanosciences UV/Ozone ProCleaner™) for 10 min. to create a clean, hydrophilic surface. The first PAA layer was deposited on the silicon wafer by dipping it into a 1 mg/mL solution of PAA (pH 2.96) for 10 min followed by rinsing with water (pH 2.97) for 1 min and drying in air. The thickness of this layer was measured via spectroscopic ellipsometry (VASE, J. A. Woollam Co., Inc., Lincoln, NE, USA) at three different positions.[18] In a typical scan, the wavelength was varied between 400 and 800 nm, and the angles-of-incidence were chosen to be near the pseudo-Brewster angle of silicon (ranging from 70 to 76 degrees). The analysis considered the thickness

of the silicon's native oxide (2.4 ± 0.7 nm), which was measured in a separate experiment. The mean thickness and standard deviation were calculated across the area of the beam's footprint (approximately 3 mm x 8 mm).

A layer of MPTS-PEG1 nanoparticles was deposited by placing approximately 1 mL of a 0.32 mg/mL dispersion (pH 2.97) on the surface for 10 min. with subsequent rinsing with water (pH 2.97) for 1 min. and drying in air. All subsequent layers were deposited in a similar way and the thickness of the multi-layer was measured after each deposition after drying the samples in air. For comparison, multi-layer coatings were also made by alternately depositing MePEG and PAA solutions onto silicon wafers.

Ellipsometry data were analyzed by fitting to a slab model.[19] The refractive indices of each layer were determined through independent measurements on thick films deposited in separate experiments, and these values were used in modeling the multi-layer data. The effects of thickness non-uniformity were included in the model. The thickness value obtained from measurements of the first layer thickness was used in the model for the second layer, and so on for the third and following layers.

2.14. Fluorescence microscopy. Fluorescently-labeled nanoparticles were used to build multilayered materials using the above-described layer-by-layer deposition protocol. Fluorescence microscopy was performed on fluorescence microscope (Zeiss, Imager.A1) with AxioCam MRm Zeiss camera at 10× magnification and an exposure time of 250 μs. Each image contained 1388 ×1040 pixels.

2.15. Scanning electron microscopy (SEM). Experiments used an FEI Quanta FEG 600 environmental scanning electron microscope with an acceleration voltage of 20 kV. The surface of samples was sputtered with chromium (~10 nm thickness) before analysis.

2.16. Transmission electron microscopy (TEM). TEM images of thiolated and PEGylated nanoparticles were acquired using a Philips CM20 Analytical TEM at 80 kV accelerating voltage. For sample preparation, the carbon-coated Cu grids were brought into contact with aqueous dispersions of nanoparticles for 60 s, followed by exposure to 1 wt % uranyl acetate solution for 30 s and then dried off with a filter paper.

3. RESULTS AND DISCUSSION

3.1. Synthesis and properties of PEGylated nanoparticles

A series of PEGylated nanoparticles were synthesized by reacting thiolated MPTS-based nanoparticles with various quantities of methoxypolyethylene glycol maleimide (MePEG). These nanoparticles were characterized by dynamic light scattering and zeta-potential measurements to determine their size distribution and surface charge; and by Ellman's assay and thermal gravimetric analysis to quantify the content of thiol groups and MePEG chains, respectively. The characteristics of these nanoparticles are summarized in Table 1. The numerical suffix in the sample name indicates the MePEG quantity. Figure 1 shows the particle size distributions determined by dynamic light scattering, which are perfectly monomodal before and after PEGylation. The size of nanoparticles increases with PEGylation from 51.0±0.2 nm for the parent thiolated nanoparticles up to 75.0 ±1.5 nm for the nanoparticles synthesized with the highest content of MePEG in the reaction mixture, which is related to the formation of MePEG corona. An increase in the MePEG content in the reaction mixture results in nanoparticles of

greater size and also leads to the reduction of the thiol group content as well as to an increase in the MePEG quantity covalently attached to organosilica surface, indicating that the levels of PEGylation can be varied. Prior to PEGylation the thiolated nanoparticles showed excellent colloidal stability in aqueous dispersions within one month[16] at pH 5.8±0.1 and this is likely to be due to their electrostatic stabilization as the value of zeta-potential is highly negative (-41.97±0.50 mV). However, the storage of the thiolated nanoparticles in aqueous dispersions at 5 ºC in a refrigerator for 6 months has resulted in their partial precipitation. The TEM image of thiolated nanoparticles (inset in Figure 1) shows the presence of both non-aggregated and aggregated particles in solution, which is in good agreement with our previous report.[16] The aggregation of thiolated nanoparticles is likely to be resulting from inter-particle disulfide bond formation caused by sample drying during its preparation for TEM measurements. A PEGylation of thiolated nanoparticles results in a marked drop in zeta-potential values down to -9.26±1.10 mV, whilst their aggregative stability increases. The PEGylation of nanoparticles leads to a decrease in PDI values from 0.218±0.010 to 0.107±0.010, indicating that the nanoparticles are less polydisperse and less prone to form aggregates. The PEGylated nanoparticles did not show any signs of precipitation during 6 months of storage at 5 ºC and their TEM image indicates the presence of non-aggregated particles only. The colloidal stability of PEGylated nanoparticles is likely to be the result of steric factors ensured by the high hydrophilicity of the MPEG-based corona.

Table 1. Characteristics of nanoparticles before and after PEGylation

Sample	MePEG	Z-size,	PDI	Z-potential,	SH-group	MePEG

	quantity in reaction mixture, mg/mL	nm		mV	content, μmol/g	content*, μmol/g
MPTS	0	51.0±0.2	0.218±0.010	-41.97±0.50	137±6	0
MPTS-PEG 1	5	65.0±0.8	0.120±0.010	-14.23±0.20	58±6	8**
MPTS-PEG 2	10	70.0±0.8	0.115±0.020	-11.70±0.90	47±1	16
MPTS-PEG 3	20	75.0±1.5	0.107±0.010	-9.26±1.10	17±1	33

*Calculated based on TGA data; **This result was calculated by extrapolation as MPTS-PEG1 sample was not available for TGA.

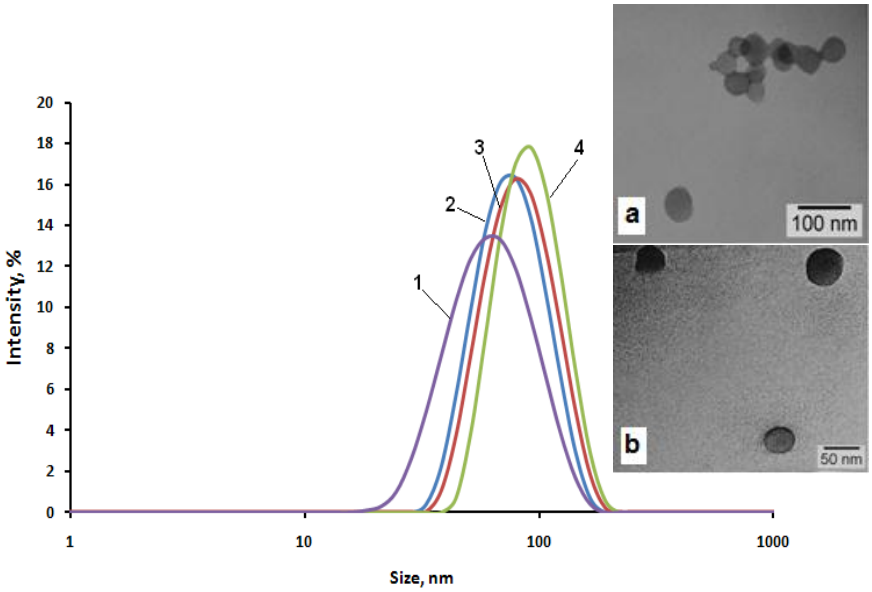

Figure 1. Size distribution for nanoparticles before and after PEGylation as measured by DLS. MPTS nanoparticles (1), MPTS-PEG1 (2), MPTS-PEG2 (3), and MPTS-PEG3 (4). Insets: TEM images of MPTS (a) and MPTS-PEG1 (b) nanoparticles

Previously, we discussed the excellent potential for thiolated and PEGylated nanoparticles for drug delivery.[16] However, the use of nano-carriers in drug delivery via different routes of administration may involve their exposure to media over a range of pH values. For example, when nanoparticles are administered orally, they will travel through the various regions of the gastrointestinal tract having drastically different pHs (around pH 2 in the stomach and pH 6-7 in the small intestine).[20] Therefore, we evaluated the effect of pH on the size of both the thiolated and the PEGylated nanoparticles (Figure 2).

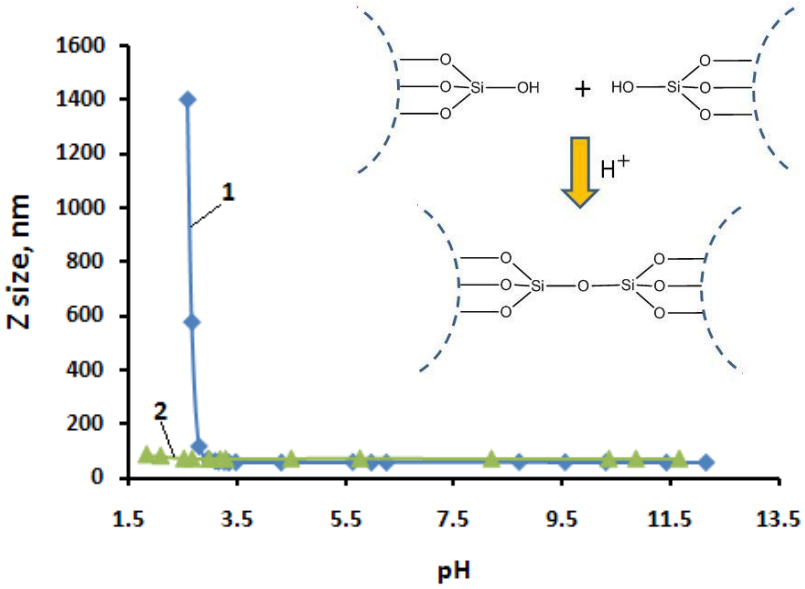

Figure 2. Z-average size of MPTS (1) and MPTS-PEG1 (2) nanoparticles as a function of solution pH. Inset: Scheme showing the formation of Si-O-Si bridges between nanoparticles under acidic conditions

The thiolated nanoparticles show excellent stability in a broad range of pHs from 3.0 to 12.0, however, at pH < 3.0 they tend to aggregate with a remarkable increase in particle size from 51

nm to 1.4 μm. This aggregation is irreversible as the nanoparticles cannot be re-dispersed after switching pH back to higher values. This irreversibility could be related to the formation of Si-O-Si covalent bridges between ≡Si-OH groups present on the surface of nanoparticles. This condensation is known to happen under acidic conditions.[21a] The PEGylated nanoparticles, on the contrary, do not aggregate at any pH. They also did not show any increase in size upon addition of up to 0.2 mol/L sodium chloride (data not shown), confirming our hypothesis about their stabilization by steric factors. Similar stabililization of silica nanoparticles after PEGylation was previously observed by Branda et al.[21b] and was likewise explained by steric factors.

3.2. Hydrogen-bonding driven self-assembly of PEGylated nanoparticles with poly(acrylic acid) in solutions

It is well known that polyethyleneglycol is capable of forming hydrogen-bonded interpolymer complexes (IPCs) with poly(acrylic acid) (PAA) in aqueous solutions under acidic conditions.[22-25] These complexes are usually formed immediately after mixing aqueous solutions of polymers. The possibility of complex formation as well as the structure of IPCs depend on the molecular weights of both PAA and PEG, their concentrations, and the solution pH. This complexation has also previously been utilized to build multilayered coatings by alternate dipping of solid substrates into solutions of PAA and PEG.[26-29.] More information on the progress in the area of layer-by-layer deposition of polymers via hydrogen bonding can be found in three reviews by the Sukhishvili and Caruso groups.[30-31]

Recently, D'Addio and co-workers[32] have reported a novel technique to purify and concentrate PEG-b-poly(lactide-co-glycolide) self-assembled nanoparticles coated with a dense layer of PEG chains by utilizing their ability to form hydrogen-bonded complexes with low

molecular weight polyacids such as poly(acrylic acid) (~1.8 kDa), poly(aspartic acid) (~ 2 kDa) and citric acid. The strong hydrogen bonding between PEG's ether groups and carboxylic groups of polyacids resulted in rapid precipitation of interpolymer coacervates, which could be easily re-dissolved at pH 7. We are not aware of any other studies reporting the interactions between PEGylated nanoparticles and poly(acrylic acid) in solutions and at solid surfaces.

The presence of MePEG on the surface of our organosilica nanoparticles also opens up an interesting opportunity for their further modification through the complex formation with poly(acrylic acid). Figure 3 shows the size distributions of aqueous solutions of PAA, PEGylated nanoparticles, their mixture as well as the mixture of PAA with linear MePEG at pH 2.96. The hydrodynamic diameter of PAA coils determined by dynamic light scattering is 48 ± 2 nm, which is in agreement with the data reported by Deng et al.[33] The macromolecules of linear MePEG had a relatively small molecular weight (5 kDa) and could not scatter laser light efficiently; therefore aqueous solutions of MePEG did not give a well defined size distribution of a good quality (data not shown). However, mixing PAA with linear MePEG resulted in IPC nanoparticles with monomodal size distribution and an average diameter of 111±2 nm. Mixing PAA solutions with dispersions of PEGylated nanoparticles also resulted in formation of larger nanostructures, whose size is greater than the diameters of individual components (PAA and MPTS-PEG1) and IPCs formed by linear polymers. The formation of larger nanostructures clearly demonstrates the existence of specific interactions between PAA and MPTS-PEG1 driven by hydrogen bonding.

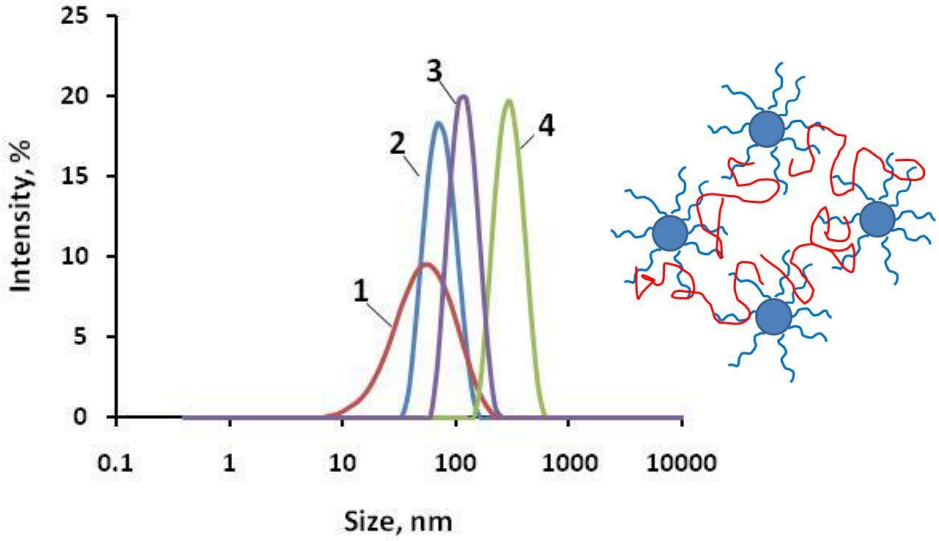

Figure 3. Size distributions for aqueous solutions of (1) PAA, (2) MPTS-PEG1, (3) PAA / MePEG complex and (4) PAA / MPTS-PEG1 complex at pH 2.96. Concentrations of PAA and MPTS-PEG1 in solutions are 1 mg/mL and 0.31 mg/mL, respectively. Complexes were prepared by mixing individual solutions in 1:1 volume ratio. The size distributions of complexes formed by PAA with MPTS-PEG2 and MPTS-PEG3 can be found in the *Supporting Information*. Inset: Proposed scheme of aggregation of PEGylated nanoparticles in the presence of PAA.

It should be noted that the formation of interpolymer complexes between PEGylated nanoparticles and PAA under acidic conditions is not prevented when up to 0.2 mol/L of NaCl was added to their solutions. Moreover, the presence of NaCl in solutions resulted in more intensive complexation and larger interpolymer aggregates formed (data not shown), which is in good agreement with our previous study reporting the salt effects on hydrogen-bonded complexes.[34] The stability of hydrogen-bonded complexes in solution with high ionic strength

makes hydrogen-bonded IPC different from polyelectrolyte complexes, which are known to dissociate at similar salt concentrations.[35]

3.3. Layer-by-layer self-assembly of PEGylated nanoparticles and poly(acrylic acid) on silicon wafers

There is currently a growing interest of researchers in the development of various multilayer composite materials incorporating inorganic and hybrid nanomaterials with functional polymers using layer-by-layer deposition on solid surfaces.[36-38] For example, Du et al.[38] have reported the development of UV-visible antireflection coatings using the electrostatic interactions between TEOS-based organosilica nanoparticles with incorporated PAA and cationic poly(allylamine hydrochloride) for deposition on poly(methyl methacrylate) and glass substrates in a layer-by-layer fashion.

We propose that the hydrogen bonding interactions between poly(acrylic acid) and MePEG chains on the surface of PEGylated nanoparticles can be used for the fabrication of multilayered coatings on a solid substrate. The advantages of hydrogen bonding interactions between polymers over electrostatic forces include the possibility of assembling the multilayered materials under acidic conditions or in media with a relatively high ionic strength. Moreover, the polymers forming hydrogen-bonded complexes, such as PAA and PEG, have excellent toxicological profiles and are widely used in biomedical and pharmaceutical applications.[20]

Here we have used silicon wafers as a model substrate because it is suitable for ellipsometry measurements to determine the thickness of multi-layer coatings. The initial experiments on layer-by-layer deposition on silica wafer surfaces were performed with fluorescently-labeled MPTS-PEG1 nanoparticles, which were synthesized in our previous study.[16] The application of

these nanoparticles in layer-by-layer deposition on silicon wafer gives an excellent opportunity to analyze the structure and uniformity of multilayers by fluorescence microscopy (Figure 4).

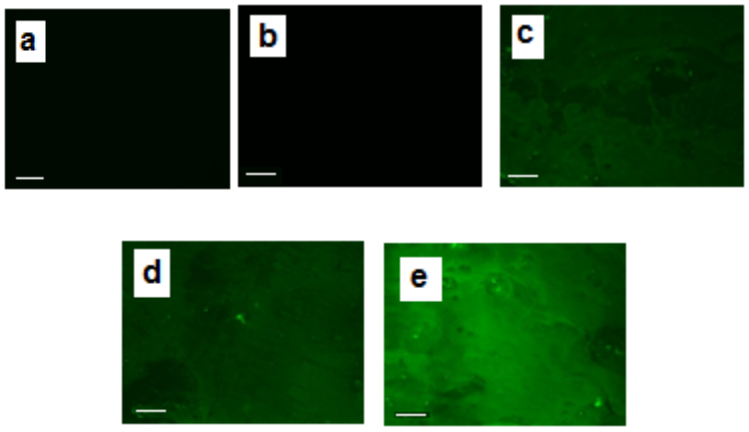

Figure 4. Fluorescent microphotograph of a silicon wafer before (a) deposition, (b) first layer of PAA, (c) first layer of nanoparticles, (d) second layer of PAA and (e) second layer of nanoparticles. Green color indicates fluorescence. Size bar is 200 μm.

As was expected, the silicon wafer and the first deposited layer of PAA do not show any signs of fluorescence. After the first layer of fluorescent nanoparticles is deposited, the wafer surface becomes fluorescent but the distribution of nanoparticles is uneven and patchy. The subsequent layer of PAA does not change the fluorescent intensity because of its possible optical transparency. A deposition of the next layer of nanoparticles results in more intensive fluorescence and its more even distribution on the surface.

Additional characterization of multilayered coatings was undertaken with the help of scanning electron microscopy (Figure 5). The SEM images demonstrate that the silicon wafer before and after coating with PAA are perfectly flat and featureless surfaces. At the levels of

magnification used, it is impossible to visualize any PAA macromolecules deposited on silicon wafer surfaces. When the first layer of MPTS-PEG1 was deposited on the top of the first layer of PAA, these nanoparticles are clearly visible as spherical objects often forming agglomerates. This layer of nanoparticles appears very patchy with incomplete coating of the surface. When the subsequent layers of PAA and MPTS-PEG1 were deposited, the extent of surface coverage with nanoparticles increases but uncoated gaps still are clearly visible. It can be expected that a complete coverage could potentially be achieved if a third layer of MPTS-PEG1 nanoparticles was deposited on the surface. It can also be hypothesized that the incomplete coverage and a "patchy" structure of coatings is related to a low concentration of deposited nanoparticles in aqueous dispersion used. Therefore, a better coating efficiency can be anticipated if more concentrated dispersions of MPTS-PEG1 are used for surface coating.

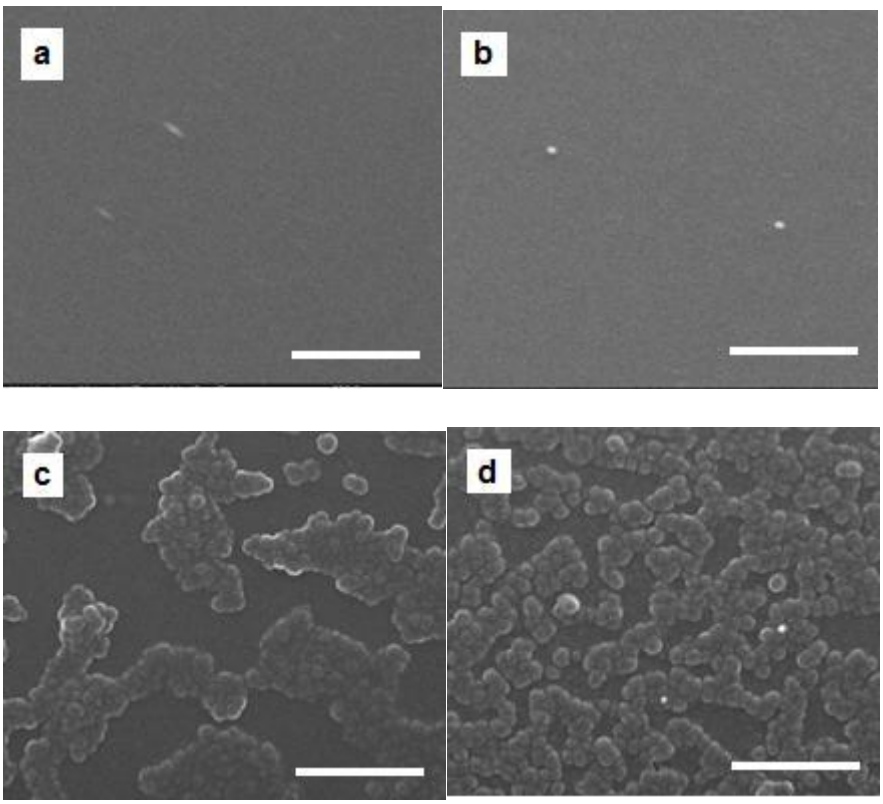

Figure 5. SEM images of the silicon wafer surface before coating (a) and after coating with the first layer of PAA (b), layers of PAA/MPTS-PEG1 (c), and layers of PAA/MPTS-PEG1/PAA/MPTS-PEG1 (d). The scale bar is 500 nm in all cases.

The microscopy results provided useful information about the non-uniform structure of coatings, which was taken into consideration for measurement of their thickness by ellipsometry. The thickness of the first deposited layer of PAA was found to be 11.8 ±1.8 nm by ellipsometry analysis (using a refractive index, n, at a wavelength of λ = 500 nm of 1.50 in the modeling, as was obtained in an independent measurement on a thicker film). Subsequently the deposition of MPTS-PEG1 on the surface resulted in a layer with an effective thickness of 24.2 ±2.0 nm (using n = 1.39 at λ = 500 nm, obtained independently). It should be noted that this thickness is much smaller compared to the diameter of nanoparticles measured by dynamic light scattering (65.0±0.8 nm). This discrepancy may be related to a number of factors. First, the measurement is sensitive to the product of the layer thickness and its refractive index; the parameters are coupled. If the density, and hence n of the monolayer, is lower than in a thick layer (where n = 1.39), the analysis would under-estimate the thickness. Void spaces between particles, with sizes smaller than the wavelength of light (up to *ca.* 100 nm) will decrease the refractive index. Secondly, there is heterogeneity in the packing of the particles, and the measurement represents only an average across the footprint of the beam. Furthermore, the size measured by dynamic light scattering in aqueous dispersion will be the diameter of fully-swollen and hydrated nanoparticles whereas the thickness of multilayers was measured by ellipsometry in the dry state. The next layer of PAA deposited on the top of nanoparticles showed an effective thickness of 5.8 ±4.5 nm. The pattern of thickness increase is presented in Figure 6. Despite the limitations of the

measurement of this non-ideal system, ellipsometry is suitable for the characterization of thickness increase during the build-up of multilayers and for the comparison of materials systems.

To gain a better insight into the formation of MPTS-PEG / PAA multilayers, we have also studied the layer-by-layer deposition of linear PAA and MePEG. Figure 6 compares the cumulative thicknesses of MePEG/PAA multilayers to of MPTS-PEG1/PAA, as a function of a number of monolayers (depositions). It is apparent that the multilayers containing the silica nanoparticles (MPTS-PEG1) are consistently thicker. Both systems show a step-like increase in thickness. The MPTS-PEG1 layers are consistently thicker than the PAA layers, whereas the PAA layers are consistently thicker than the MePEG layers.

The thickness values for MePEG/PAA multilayers are in rough agreement with the data reported by Kharlampieva and Sukhishvili.[30a] For example, they reported that the thickness of the first poly(ethylene oxide)/poly(acrylic acid) bi-layer is around 10 nm and the second bi-layer is around 15 nm. However, a direct comparison of these results is not fully possible because of the differences in polymer molecular weights, deposition conditions, and the nature of the substrate. The formation of coatings involving nanoparticles results in a much faster thickness growth. This is also expected bearing in mind the larger size of these nanoparticles compared to linear MePEG. Previously, Seo et al.[39] have also observed a higher rate growth of multilayer thickness (*i.e.* thicker layers) for complexes of hydrophobically-modified poly(ethylene oxide) (PEO) and PAA compared to the unmodified PEO / PAA system. However, this effect was observed when the number of monolayers exceeded 10. This result was explained by the authors[37] by involvement of hydrophobically-modified PEO in the layer-by-layer self-assembly in the form of larger micellar aggregates.

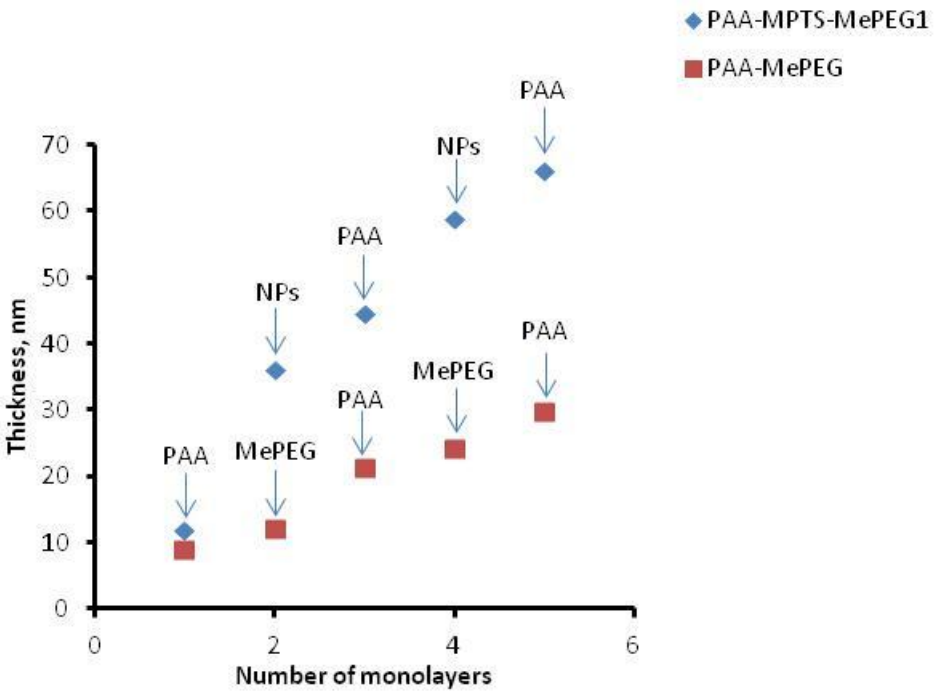

Figure 6. Thickness of multilayers determined by ellipsometry as a function of the number of monolayers. Here, NPs refer to nanoparticles of MPTS-MePEG1.

In a separate set of experiments, we have evaluated the thickness of MPTS-PEG1 nanoparticles and MePEG deposits on silicon wafer surfaces with and without a prior deposition of PAA (Figure 7). The thickness of the nanoparticles layer directly deposited on the oxidized silicon surface is significantly lower compared to the value when they are deposited onto the first PAA layer. This difference can be explained by the greater affinity between PEGylated nanoparticles and PAA compared to the affinity with oxidized silicon, which results in an increased surface coverage and greater thickness values. This affinity is a result of the hydrogen bond formation between the carboxylic groups of PAA and the oxygen in the ethylene glycol repeat units. In contrast, MePEG did not show any significant difference in the thickness when deposited with or

without the layer of PAA. Perhaps this is related to the small size of MePEG macromolecules which makes any difference within the resolution of these particular ellipsometry measurements, whereas the MPTS-PEG1 particles constitute larger "building blocks" in the structure.

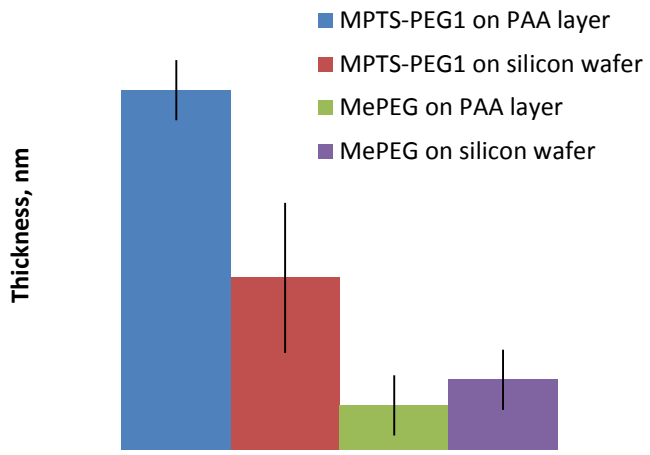

Figure 7. Thickness of MPTS-MePEG1 and MePEG layers deposited onto surfaces of silicon wafer, both with and without a PAA layer.

The analysis of ellipsometry results coupled with the data from fluorescent and scanning electron microscopy allow us to propose the following descriptive model for the deposition of PAA and PEGylated nanoparticles on silicon wafer surfaces (Figure.8). The first layer of nanoparticles deposits on PAA-coated surface and forms a very patchy coating with approximately 50 % of the surface being covered. In the subsequent depositions of PAA and MPTS-PEG1, the nanoparticles fill into the voids of the first layer and also create an incomplete second layer.

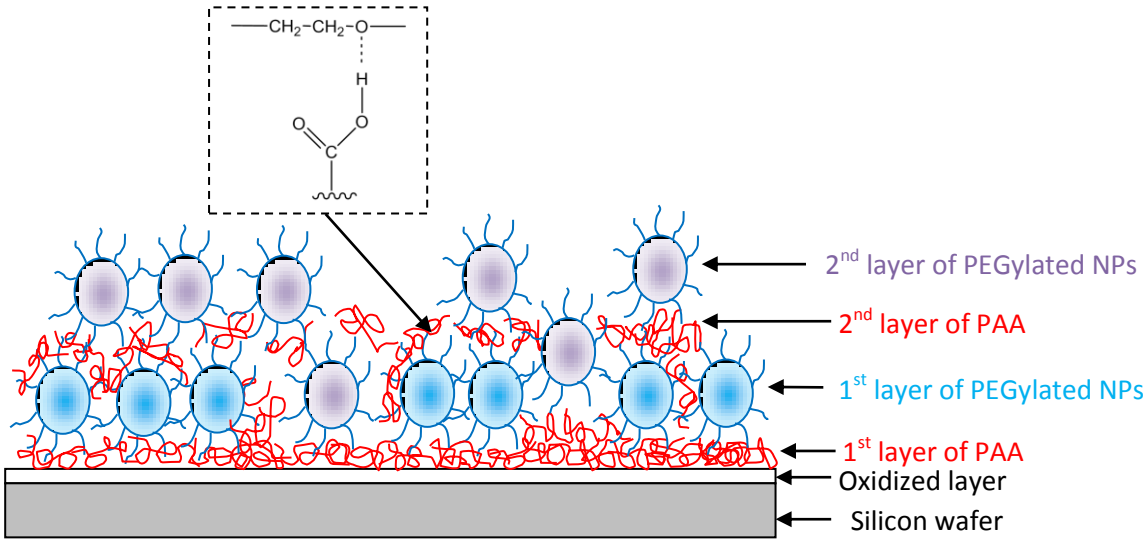

Figure 8. Proposed scheme of PEGylated nanoparticles (NPs) – poly(acrylic acid) layer-by-layer self-assembly at silicon wafer surfaces. The second layer of PEGylated NPs is shown in different color for clarity of presentation. Inset shows the scheme of hydrogen bonding between carboxylic groups of PAA and ether groups of MePEG.

4. CONCLUDING REMARKS

Thiolated organosilica nanoparticles were successfully PEGylated by reacting with methoxypolyethylene glycol maleimide. The levels of nanoparticle PEGylation can be easily controlled by varying the quantity of methoxypolyethylene glycol maleimide in the reaction mixture. The PEGylated nanoparticles showed excellent colloidal stability over a wide range of pHs, whereas their parent thiolated nanoparticles underwent irreversible aggregation at pH < 3.0. The presence of PEG functionality on the surface of PEGylated nanoparticles allows their further modification through hydrogen-bonding assembly with poly(acrylic acid) under acidic pH conditions. When this self-assembly was performed in solutions, it results in the formation of

larger nanostructures, whereas when it was realized at silicon wafer surface using a layer-by-layer deposition approach, it leads to multilayered coatings. The rate of the thickness growth for multilayers involving the PEGylated nanoparticles is greater compared to the complexes between linear poly(acrylic acid) and methoxypolyethylene glycol. The layer-by-layer assembly involving PEGylated nanoparticles allows their more efficient attachment to the surfaces mediated by hydrogen bonding with poly(acrylic acid). When these nanoparticles are fluorescently-labeled, their layer-by-layer assembly results in the development of fluorescent surfaces.

PEGylated nanoparticles have attracted the attention of pharmaceutical researchers in the past few decades due to the numerous advantages offered by these systems for drug delivery. PEGylation of nanoparticles is known to enhance their circulation time in the blood stream by inhibition of nonspecific protein adsorption,[40] and it also may facilitate the diffusion through the mucus network for nanomedicines administered via mucosal routes.[41] The hydrogen bonding-driven interactions between PEGylated nanoparticles and other water-soluble polymers in aqueous dispersions may have important implications in pharmaceutical formulations containing complex mixtures. Strong interactions resulting in the formation of interpolymer complexes, as in the case of MPTS-PEG / poly(acrylic acid) studied in this work, should be taken into consideration when formulating these systems. These interactions may occur in pharmaceutically-relevant formulations, when drug-containing PEGylated nanoparticles are dispersed in weakly-cross-linked commercial derivatives of poly(acrylic acid) such as Carbopols®, which are often used for formulating gels for topical applications. Furthermore, these interactions may hamper the diffusion of PEGylated nanoparticles through Carbopol® gels. Consequently, the pH-responsiveness of the hydrogen bonds between ether groups of PEGylated nanoparticles and carboxylic acids of Carbopol® could be exploited when designing systems with the pH-triggered release of these nanoparticles.

From this perspective, the possibility of utilizing layer-by-layer deposition of PEGylated nanoparticles and poly(acrylic acid) on the surface of pharmaceutical micro-particulate carriers may also offer a novel approach for designing drug delivery systems with a complex multi-stage and pH-triggered release profile.

ACKNOWLEDGEMENTS

GSI is grateful to the Bolashak Foundation (Kazakhstan) for providing an international scholarship grant. Chemical Analysis Facility (University of Reading) is acknowledged for providing access to thermal gravimetric analysis. The help of Dr C. Stain (Centre for Advanced Microscopy, University of Reading) in SEM experiments is greatly appreciated. Special thanks are extended to Mr S. Pountney for help with fluorescent microscopy, to Ms Ellina Mun and Dr Olga Khutoryanskaya for help with thermal gravimetric analysis, and to Prof. J. Lawrence and Dr. L. Kudsiova (King's College London) for support in zeta-potential measurements.

SUPPORTING INFORMATION AVAILABLE

Additional data on thermal analysis of MPTS-PEG and particle size distributions for PAA / MPTS-PEG complexes. This information is available free of charge via the Internet at http://pubs.acs.org.

AUTHOR INFORMATION

Dr Vitaliy V. Khutoryanskiy, Reading School of Pharmacy, University of Reading, Whiteknights, P.O. Box 224, RG6 6AD Reading, United Kingdom. Fax: +44 (0) 118 378 4703; Tel: +44 (0) 118 378 6119; E-mail: v.khutoryanskiy@reading.ac.uk.

REFERENCES

(1) Lim, M.H.; Blanford, C.F.; Stein, A. *Chem. Mater.* **1998**, 10, 467.

(2) Dabre, R.; Schwammle, A.; Lammerhofer, M.; Lindner, W. *J. Chromatography A* **2009**, 1216, 3473.

(3) Nakamura, M.; Ozaki, S.; Abe, M.; Doi, H.; Matsumoto, T.; Ishimura, K. *Colloids Surf. B.* **2010**, 79, 19.

(4) Prestidge, C.A.; Barnes, T.A.; Lau, C.-H.; Barnett, C.; Loni, A.; Canham, L., *Expert Opin. Drug. Deliv.* **2007**, 4, 101.

(5) Stober, W.; Fink, A.; Bohn, E. *J. Colloid Interf. Sci.* **1968**, 26, 62.

(6) Shyjumon, I.; Rappolt, M.; Sartori, B.; Cacho-Nerin, F.; Grenci, G.; Laggner, P.; Amenitsch H. *Langmuir* **2011**, 27, 5542.

(7) Nakabayashi, H.; Yamada, A.; Noba, M.; Kobayashi, Y.; Konno M.; Nagao D. *Langmuir* **2010**, 26, 7512.

(8) Branda, F.; Silvestri, B.; Luciani, G.; Costantini, A. *Colloids Surf. A.* **2007**, 299, 252.

(9) Kozlova, N.; Santore, M.M. *Langmuir* **2006**, 22, 1135.

(10) Sadasivan, S.; Khushalani, D.; Mann, S. *J. Mater. Chem.* **2003**, 13, 1023.

(11) Mori, Y.; Pinnavaia, T.J. *Chem. Mater.* **2001**, 13, 2173.

(12) Billinge, S.J.L.; McKimmy, E.J.; Shatnawi, M.; Kim, H.J.; Petkov, V.; Wermeille, D.; Pinnavaia, T.J. *J. Am. Chem. Soc.* **2005**, 127, 8492.

(13) Hall, S.R.; Fowler, C.E.; Lebeau, B.; Mann, S. *Chem. Comm.* **1999**, 201.

(14) Nooney, R.I.; Thirunavukkarasu, D.; Chen, Y.; Josephs, R.; Ostafin, A.E. *Chem. Mater.* **2002**, 14, 4721.

(15) Moller, K.; Kobler, J.; Bein, T. *Adv. Funct. Mater.* **2007**, 17, 605.

(16) Irmukhametova, G.S.; Mun, G.A.; Khutoryanskiy, V.V., *Langmuir* **2011**, 27, 9551.

(17) Bravo-Osuna, I.; Teutonico, D.; Arpicco, S.; Vauthier, C.; Ponchel, G. *Int. J. Pharm.* **2007**, 340, 173.

(18) Keddie, J.L. *Curr. Opin. Colloid Interf. Sci.* **2001**, 6, 102.

(19) Nerapusri, Keddie, J.L.; Vincent, B.; Bushnak I.A. *Langmuir* **2006,** 22, 5036.

(20) Hillery, A.M.; Lloyd, A.W.; Swarbrick, J. Drug Delivery and Targeting for Pharmacists and Pharmaceutical Scientists, CRC Press **2001**, 475.

(21) (a) Grubb, W.T. *J. Am. Chem. Soc.* **1954**, 76, 3408; (b) Branda, F.; Silvestri, B.; Luciani, G.; Tescione, F. *Colloid. Surf. A* **2010**, 367, 12.

(22) Bailey, F. E.; Lundberg, R. D.; Callard, R. W. *J. Polym. Sci., Part A* **1964**, *2*, 845.

(23) Ikawa, T.; Abe K.; Honda, K.; Tsuchida, E. *J. Polym. Sci.: Polym. Chem. Ed.* **1975**, *13*, 1505.

(24) Staikos, G.; Antonopoulou, P.; Christou, E. *Polym. Bull.* **1989**, *21*, 209.

(25) Khutoryanskiy, V.V.; Dubolazov, A.V.; Nurkeeva, Z.S.; Mun, G.A. *Langmuir* **2004**, 20, 3785.

(26) Lutkenhaus, J.L.; Hrabak, K.D.; McEnnis, K.; Hammond, P.T., *J. Am. Chem. Soc.* **2005**, 127, 17228.

(27) Lutkenhaus, J.L.; McEnnis, K.; Hammond, P.T., *Macromolecules* **2007**, 40, 8367.

(28) Seo, J.; Lutkenhaus, J.L.; Kim, J.; Hammond, P.T.; Char, K., *Langmuir* **2008,** *24*, 7995.

(29) Sukhishvili, S.A.; Granick, S. *Macromolecules* 2002, 35, 301.

(30) (a) Kharlampieva, E.; Sukhishvili, S. *J. Macromol. Sci. Polym. Rev.,* **2006**, 46, 377. (b) Kharlampieva, E.; Kozlovksaya, V.; Sukhishvili, S.A. *Adv. Mater.* **2009**, 21, 3053.

(31) Such, G.K.; Johnston, A.P.R.; Caruso, F. *Chem. Soc. Rev.* **2011**, 40, 19.

(32) D'Addio, S.M.; Kafka, C.; Akbulut, M.; Beattie, P.; Saad, W.; Herrera, M.; Kennedy, M.T.; Prud'homme, R.K. *Molecular Pharmaceutics* **2010**, 7, 557.

(33) Deng, L.; Wang, C.; Li, Z.-C.; Liang, D. *Macromolecules* **2010**, 43, 3004.

(34) Khutoryanskiy, V.V.; Mun, G.A.; Nurkeeva, Z.S.; Dubolazov, A.V. *Polym. Int.* **2004**, 53, 1382.

(35) Khutoryanskiy, V.V.; Nurkeeva, Z.S.; Mun, G.A.; Sergaziyev, A.D.; Ryskalieva, Zh.; Rosiak, J.M. *Eur. Polym. J.* **2003**, 39, 761.

(36) Srivastava, S.; Kotov, N.A. *Acc. Chem. Res.* **2008**, 41, 1831.

(37) Lutkenhaus, J.L; Olivetti, E.A.; Verploegen, E.A.; Cord, B.M.; Sadoway, D.R.; Hammond, P.T. *Langmuir*, **2007**, 23, 8515.

(38) Du, Y.; Luna, L.E.; Tan, W.S.; Rubner, M.F.; Cohen, R.E. *ACS Nano* **2010**, 4, 4308.

(39) Seo, J.; Lutkenhaus, J.L.; Kim, J.; Hammond, P.T.; Char, K. *Macromolecules* **2007**, 40, 4028.

(40) Park, J.; Fong, P.M.; Lu, J.; Russell, K.S.; Booth, C.J.; Saltzman, W.M.; Fahmy, T.M. *Nanomedicine: Nanotechnol. Biol. Med.* **2009**, 5, 410.

(41) (a) Yoncheva, K.; Lizarraga, E.; Irache, J.M. *Eur. J. Pharm. Sci.* **2005**, 24, 411.

(b) Wang, Y.-Y.; Lai, S.K.; Suk, J.S.; Pace, A.; Cone, R.; Hanes, J. *Angew. Chem. Intl.* **2008**, 47, 9726.

Published in *Langmuir* (2012) **28**: 299-306

TOC Graphic